Sequential Hybrid Approach for Reliable Detection of Rainfall Pauses at the Beginning of the Rainy Season in Senegal: Towards a Predictive Tool for False Starts

Pape El Hadji Abdoulaye Gueye[1], Cherif Bachir Deme[1], and Adrien Basse[1]

University Alioune Diop, Bambey, Senegal
{papeabdoulaye.gueye, cherifbachir.deme, adrien.basse}@uadb.edu.sn

Abstract. This work focuses on the detection of false onsets of the rainy season in Senegal, a critical factor that can lead farmers, particularly smallholders, to initiate agricultural activities prematurely. Such errors, caused by misleading early rainfall events, result in yield losses and increase farmers' vulnerability to climate variability. Unlike existing methods, our approach incorporates statistical tests (such as Pettitt, Kendall, and Lombard) to enrich the input dataset with relevant change points related to rainfall, soil moisture, and vegetation. This enrichment step, combined with a formal detection of false onsets based on climatic, phenological, and statistical criteria, enhances the relevance, robustness, and contextualization of detection compared to purely statistical or physical approaches. In this context, a deep learning methodology was developed to identify false onsets at an early stage using multivariate climatic data. We designed a hybrid model combining LSTM, GRU, and multi-head attention layers to extract complementary representations of the input sequence. This architecture integrates long-term memory (LSTM), short- to mid-term sequence representation (GRU), and cross-temporal relationships (attention), in order to improve the detection of false onset events. Model hyperparameters were optimized through Bayesian search to enhance detection performance. Results show consistent improvements across all key metrics: accuracy increased from 0.84 to 0.88, F1-score from 0.833 to 0.86, recall remained perfect at 1.0, precision rose from 0.767 to 0.81, and AUC improved from 0.900 to 0.92. These gains demonstrate the overall robustness of the optimized model, ensuring more reliable detection of false onsets. The findings highlight the importance of hyperparameter optimization in strengthening the predictive capacity of hybrid models. They also emphasize the value of multi-faceted evaluation combining performance metrics, interpretability methods (e.g., SHAP), and robustness analyses, leading to a reliable, interpretable, and operationally relevant detection framework for false onsets of the rainy season.

Keywords: False onset; Deep learning; Statistical tests; Hybridization (LSTM, GRU, Attention); Bayesian optimization

1 Introduction

In semi-arid regions, particularly in the Sahel, agricultural drought — defined as a water deficit affecting crops and their productivity — constitutes a major risk to food security [1]. This region, and notably Senegal, is characterized by strong interannual rainfall variability [2], frequent delays in the onset of the rainy season, an extended dry season, and a continuous increase in land surface temperature (LST) [3, 4]. These climatic changes disrupt traditional agricultural cycles and increase the vulnerability of rainfed production systems. In this context, the *false onset* of the rainy season is a critical factor. It occurs as a series of weak initial rains — or sometimes a total of about 20 mm over 2–3 days — followed by a dry spell. This phenomenon creates a false sense of security for farmers, who may sow prematurely, exposing their crops to water stress that can significantly reduce yields. Despite extensive research on drought detection, the false onset — a key factor in shifting the rainfall calendar — has received relatively little attention, limiting the predictive capabilities of existing models [5]. Early detection is therefore essential to adjust sowing schedules, mitigate water stress risks, and support farmers' decision-making. The objective of this work is to define and predict a *false onset index* of the rainy season in Senegal, aiming to improve the reliability of rainfall forecasts and assist farmers in planning their sowing schedules. To this end, we leverage multisource climatic data to enable early detection of such events. Our approach differs from previous work by integrating statistical tests (Pettitt, Kendall, Lombard), which enrich the dataset by identifying relevant change points in rainfall, soil moisture, and vegetation. Additionally, the false onset is formally defined using climatic, phenological, and statistical criteria, ensuring a more robust, contextualized, and realistic detection compared to previous methods. Finally, this paper is organized as follows. Section 2 reviews related work. Section 3 describes the dataset, the LSTM–GRU–Transformer hybrid model, and the hyperparameter optimization. Section 4 presents the results, including performance evaluation, robustness analysis, SHAP-based interpretability, and ablation studies. Section 5 discusses the relevance, limitations, and future research directions. Finally, Section 6 concludes by highlighting the main contributions and implications of this study.

2 Related Work

2.1 Remote Sensing and Drought Indices

In recent years, remote sensing has emerged as a key tool for drought monitoring, providing continuous spatio-temporal data despite the scarcity of *in situ* measurements [4]. Indices such as NDVI, VHI, LSWI, and more recently Sun-Induced Chlorophyll Fluorescence (SIF), allow detection of vegetation water stress [6, 7, 8, 9]. Additionally, composite indices that integrate precipitation, temperature, soil moisture, and remote sensing data have proven useful, such as the CDI [10], SMADI [11], or IDSI [12].

2.2 Machine Learning and Drought Forecasting

Machine learning models have been widely developed for drought detection and forecasting. When incorporating physical constraints, they can achieve high predictive accuracy [13, 9]. Explainable AI (XAI) methods also help highlight the differentiated roles of climatic variables, with temperature sometimes being more influential than precipitation [1].

2.3 The Sahel Context In the Sahel, the timing of the rainy season is strongly influenced by large-scale climate phenomena such as ENSO. Kohonen models have been used, for example, to classify the onset and offset of the season [5]. However, these approaches have not been applied to detecting false starts of the rainy season or forecasting them. The statistical model proposed by Salack et al. [14], based on logistic regression using climate predictors (SST, precipitable water, dew point temperature, winds), shows reasonable predictive capacity at some sites (Dano, Bolgatanga) but has interregional limitations (low correlations at Bakel) and low adaptability to complex intra-seasonal dynamics.

2.4 Recurrent Neural Network Approaches LSTM networks have been applied in various hydrological and climate contexts. For instance, a multi-basin LSTM approach has been proposed for hydrological forecasting using meteorological time series (CAMELS dataset), conditioning predictions on basin static features, enabling generalization to unobserved sites [15]. In remote sensing applications, Balti et al. [16] showed that LSTMs outperform traditional methods in modeling spatio-temporal drought dynamics from satellite imagery.

2.5 Seasonal Forecasting and Explainable Models Interpretable machine learning approaches have also been explored for rainfall forecasting. For example, the SciSimple study [17] uses CHIRPS, ERA5, and ECMWF data, and evaluates algorithms such as LASSO and Elastic Net to predict seasonal anomalies (MAM, JJAS, OND) using metrics such as MBSS. These works emphasize the importance of predictor selection and data quality in forecasting models.

2.6 Hybrid Architectures for Drought More recently, hybrid architectures have been proposed to leverage heterogeneous data. Agudelo et al. [18] combine meteorological time series, static soil data, and categorical variables in an architecture integrating LSTM, FFNN, embeddings, and an attention mechanism. This approach allows predicting USDM drought categories and detecting short episodes, including those occurring after an apparent rainy season onset, a critical issue in the Sahel. However, the approach relies on rich and structured data, which can be difficult to obtain in West African contexts.

2.7 Limitations and Justification of Our Approach Existing studies show that statistical approaches have limited capacity for interregional false-start forecasting, while recurrent neural networks are better suited to capture complex spatio-temporal dynamics. However, each architecture has its limitations: LSTM excels at long-term dependencies [19], GRU is more robust to short-term variations [20], and Transformers can capture non-local relationships. Therefore, this work proposes a hybrid neural architecture combining LSTM, GRU, and Transformer to detect early false starts of the rainy season. This complementarity better represents the complexity of climate dynamics, improves seasonal onset forecasting, and optimizes the sowing calendar.

3 Materials and Methods

The data used come from multiple sources and formats, harmonized to build a consistent dataset covering the period 2000–2016. They include precipitation (CHIRPS, 5 km), air temperature, humidity, radiation, and wind (POWER-DAV, 0.5°), soil moisture, evapotranspiration, and net radiation (FLDAS, 25 km), NDVI and land surface temperature (MODIS, 1 km), as well as the drought index (SPEI) and the El Niño Oscillation (ONI). All data were aggregated over Senegal and the rainy season to obtain a representative annual value. In the dataset, false rainy season onsets were detected automatically using a simple rule based on relevant climate criteria. Specifically, the column `faux_demarrage` is set to 1 when the cumulative precipitation exceeds 600 mm and the season start date is either too early ($sos\_doy < 145$) or too late ($sos\_doy > 180$), or when July shows significant water stress, measured by SPEI (`SPEI_1_July` < -1). Otherwise, the column is set to 0. This automated detection enriches the dataset and provides input for the false start detection model. To ensure robustness, statistical tests were applied to precipitation and temperature. The Pettitt test was used to detect change points in the precipitation series. The Lombard test quantified the influence of extreme values on the distribution. Kendall's tau evaluated the association between temperature trends and false starts. The results of these tests were added as supplementary variables to improve the detection of false rainy season onsets.

3.1 Training Parameters and Hybrid LSTM-GRU-Transformer Model Configuration

We designed a hybrid model combining:

- an LSTM to capture sequential dependencies,
- a GRU to model complementary temporal patterns,
- a Transformer to extract complex relationships within sequences.

The outputs of these layers are concatenated and fed into a final dense layer with a *sigmoid* activation for binary classification.

Hyperparameter Optimization

Optimization was performed using Bayesian search with Keras Tuner. Keras

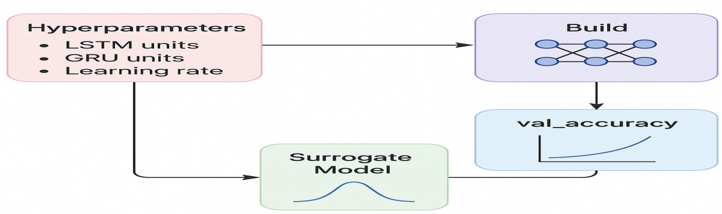

Fig. 1: KerasTuner operation for best settings

Tuner optimizes hyperparameters through the following steps: (1) **Initialization**: the surrogate model (often a Gaussian Process) is built with initial mean and standard deviation, and a few random trials are performed; (2) **Observation**: for each proposed hyperparameter combination, the model is built, trained on the training data, and evaluated on the validation data, providing the performance (val_accuracy); (3) **Update**: the surrogate model is updated with the new point (hyperparameters, val_accuracy), adjusting its predictions and uncertainty; (4) **Next trial selection**: the acquisition function (e.g., Expected Improvement) is maximized to choose the next point, balancing exploitation and exploration; (5) **Iteration**: steps 2–4 are repeated until reaching the maximum number of trials (max_trials), with each evaluation progressively guiding the search toward optimal hyperparameters. Tuned hyperparameters included the number of LSTM and GRU units, the number of Transformer heads and key dimensions, as well as the learning rate. Cross-validation (20% of the training set) ensured model robustness. The optimized hybrid model combines three com-

Table 1: Hyperparameters before and after Bayesian optimization

Hyperparameter	**Initial Value**	**Optimized Value**
LSTM units	32	16
GRU units	32	48
Number of heads	4	2
Key dimension	8	4
Learning rate	0.001	2.04×10^{-4}

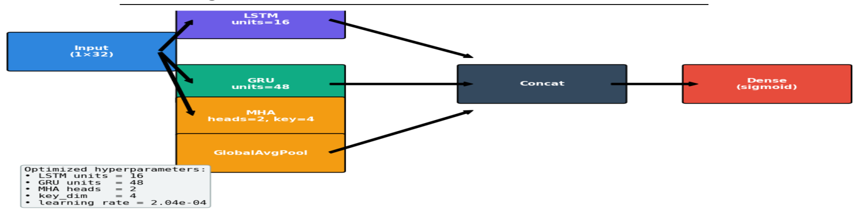

Fig. 2: Optimized model architecture

plementary branches processing the same input sequence (timestep × features) (Fig. 2). The **LSTM** branch (16 units) captures long-term dependencies using its explicit memory. The **GRU** branch (48 units) extracts short- to medium-term regularities with a simpler forget mechanism, useful for noisy signals and rapid transitions. The **Transformer** branch applies *Multi-Head Attention* (2 heads, key_dim = 4) followed by *GlobalAveragePooling* to highlight non-local relationships across sequence timesteps and produce a robust aggregate. The three representations are concatenated and passed to a *Dense* sigmoid layer, which outputs the probability of a false start. The **Adam** optimizer with a learning rate of 2.04×10^{-4} stabilizes training while maintaining AUC, and the parallel architecture (LSTM+GRU+Attention) balances long-term memory, fast dynamics, and non-local interactions, jointly improving *accuracy*, *recall*, and *F1-score*. This model enables early detection of *false start risk* at the beginning of the rainy season, thereby improving agricultural planning and resilience to climate variability.

4 Results

4.1 Data Preparation

The data come from our tabular dataset for false start detection, with `faux_demarage` as the target variable and physical variables (such as `PRECTOTCORR_SUM` and `T2M`) as predictors. The data were normalized using a *StandardScaler* to prevent dominance of certain variables, and then split into training (80%) and test (20%) sets in a stratified manner to preserve a balanced distribution of positive and negative cases.

Static Cross-Validation Training A stratified 5-fold cross-validation ($k = 5$) was used to evaluate the model's generalization performance. In each iteration, the model was trained on $k-1$ folds and validated on the remaining fold, ensuring that each observation was used once for validation. Results indicate that after hyperparameter optimization, the model becomes both more accurate on average and more stable across folds.

4.2 Performance Evaluation

The metrics used to assess the model allow evaluation of its relevance from multiple perspectives. Model performance

Table 2: Comparison of performance before and after hyperparameter optimization

Metric	Before Optimization	After Optimization
Accuracy	0.84 ± 0.196	0.88 ± 0.160
AUC	0.900 ± 0.200	0.920 ± 0.180
Precision	0.767 ± 0.291	0.810 ± 0.250
Recall	1.000 ± 0.000	1.000 ± 0.000
F1-score	0.833 ± 0.211	0.860 ± 0.196

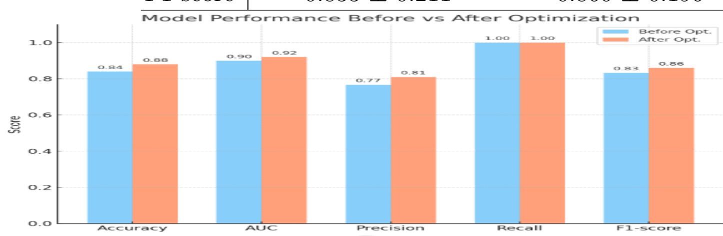

Fig. 3: Performance before and after optimization

shows improvement after hyperparameter optimization: accuracy increases from 84% to 88%, precision rises from 0.767 to 0.810, and the F1-score reaches 0.86 compared to 0.833 before optimization. Recall remains maximal (1.0), ensuring detection of all false start cases, which is essential to avoid operational errors. The AUC also improves slightly to 0.92, indicating enhanced overall discriminative ability. These results demonstrate greater robustness of the model across key metrics, confirming the effectiveness of hyperparameter optimization.

4.3 Prediction Explanation (SHAP) and Robustness

To interpret the model, SHAP kernel values were computed on 100 test cases, with 30 bootstrap samples to ensure robustness. SHAP values identify the features with the greatest impact on predictions, while the mean and standard deviation highlight both their relevance and variability, which is crucial for model interpretation and improvement.

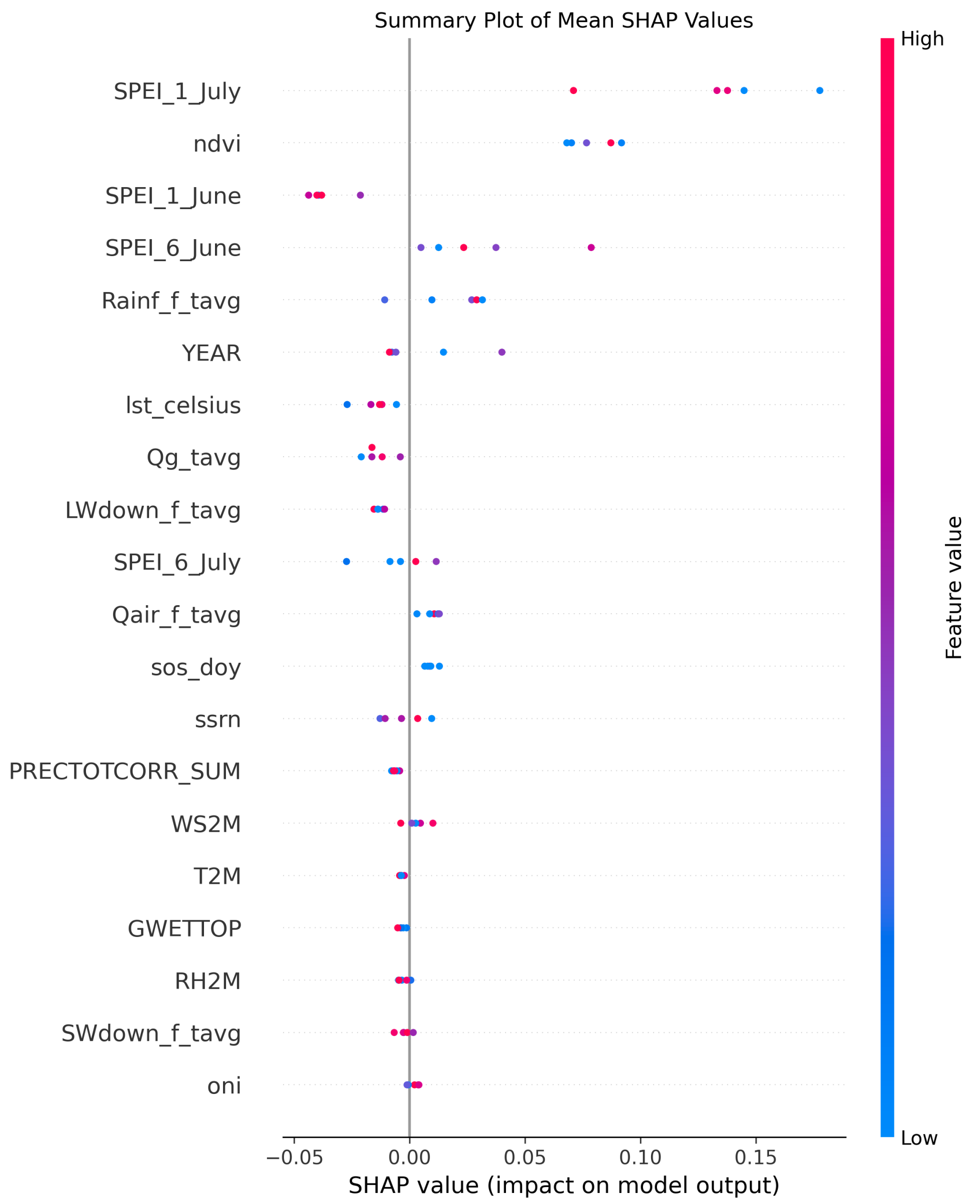

Fig. 4: Variable importance according to SHAP summary. The x-axis represents SHAP values in log-odds, showing how each feature increases or decreases the prediction.

Figure 4 shows that false starts are primarily influenced by recent hydrological indicators. In particular, `SPEI_1_July` is the most important feature at the beginning of the season, with short-term indices (`SPEI_1`) having stronger effects than longer-term six-month indices. This highlights the predominance of immediate atmospheric conditions (June–July). Composite indices such as `SPEI` are more relevant than raw precipitation (`Rainf_f_tavg`), confirming the effectiveness of synthetic water stress indicators. Global (`oni`) and phenological factors (`sos_doy`) have negligible influence, validating the predominance of local and recent causes.

4.4 Robustness via Bootstrapping

To estimate the robustness or variability of SHAP values, 30 bootstrap samples were drawn from the test set, and SHAP values were computed for each sample. The mean and standard deviation of these values provide error bars and more reliable estimates.

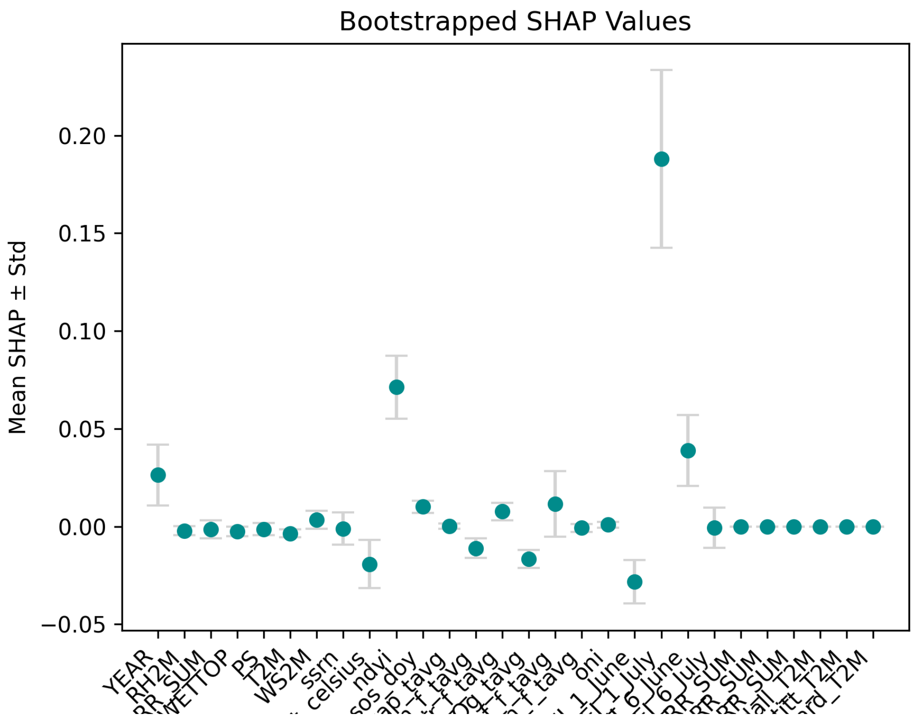

Fig. 5: Variability of SHAP values estimated via bootstrapping. Error bars reflect the standard deviation across bootstrap samples.

According to Figure 5, `SPEI_1_July` exhibits the highest mean SHAP value (+0.19), followed by `PRECTOTCORR_SUM` (+0.07). Both variables positively influence false starts during the rainy season. Bootstrapped SHAP confirms the robustness of these findings, while the relatively low standard deviation for the top features indicates consistent importance across resamples. This strengthens the understanding of underlying climatic mechanisms and provides confidence in model explanations.

4.5 Performance Evaluation Based on Timestep

The *timestep* determines the number of sequences used as model input to predict false starts.

We varied this timestep from 1 to 5 to assess its impact on model performance. Table 3 presents the mean accuracy, area under the ROC curve (AUC), precision, and F1-score (with standard deviation) across 5-fold cross-validation. According

Table 3: Performance of the LSTM + GRU + Transformer model as a function of the Timestep

Timestep	Accuracy (mean ± std)	AUC (mean ± std)	Precision (mean ± std)	F1-score (mean ± std)
1	0.84 ± 0.196	0.900 ± 0.200	0.767 ± 0.291	0.833 ± 0.211
2	0.88 ± 0.160	0.920 ± 0.180	0.810 ± 0.250	0.860 ± 0.196
3	0.86 ± 0.120	0.910 ± 0.170	0.800 ± 0.240	0.850 ± 0.190
4	0.85 ± 0.140	0.905 ± 0.180	0.795 ± 0.230	0.845 ± 0.200
5	0.83 ± 0.150	0.890 ± 0.190	0.780 ± 0.250	0.830 ± 0.210

to Table 3, the model achieves the best performance in terms of Accuracy, AUC, Precision, and F1-score when the Timestep is 2. This highlights the importance of tuning this parameter to optimize the false start detection model.

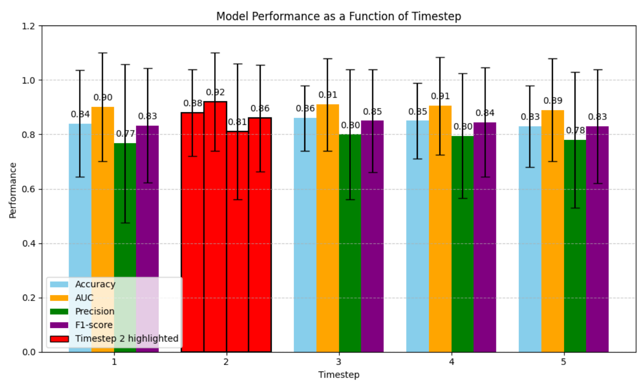

Fig. 6: Selection of the optimal timestep for the hybrid model.

Figure 6 illustrates the superiority of Timestep 2 over the others. In the following subsection, we examine the influence of different components of our hybrid model on overall performance.

4.6 Ablation Study of the Hybrid Model

To evaluate the individual contribution of the model components in predicting false starts of the rainy season, we conducted an ablation study analyzing the impact of each component on the achieved performance.

Model	Accuracy	AUC	F1-score
LSTM only	0.84 ± 0.196	0.90 ± 0.20	0.767 ± 0.291
LSTM + GRU	0.88 ± 0.16	0.92 ± 0.18	0.81 ± 0.25
LSTM + Transformer	0.86 ± 0.12	0.91 ± 0.17	0.80 ± 0.24
GRU + Transformer	0.85 ± 0.14	0.905 ± 0.18	0.795 ± 0.23
Full (LSTM + GRU + Transformer)	**0.88 ± 0.16**	**0.92 ± 0.18**	**0.86 ± 0.196**

Table 4: Ablation study of the hybrid model. Values represent mean and standard deviation over 5-fold cross-validation.

4.7 Justification of Performance

The full hybrid model (LSTM + GRU + Transformer) outperforms partial models (LSTM only, LSTM + GRU, LSTM + Transformer, GRU + Transformer) in terms of Accuracy, AUC, and F1-score. LSTM alone partially captures long-term dependencies. Adding GRU improves selective memory, enhancing recall and F1-score. Integrating the Transformer introduces an attention mechanism that helps identify critical time points, improving AUC. The combination LSTM + GRU + Transformer fully leverages the LSTM's sequential representation, the GRU's selective memory, and the Transformer's multi-head attention, providing a robust representation of the data for detecting false starts during the rainy season. We now compare our results with previous studies and present limitations and future perspectives in the following section.

5 Discussion

5.1 Main Results The study confirms the effectiveness of a hybrid model combining LSTM, GRU, and multi-head attention for detecting false starts of the rainy season. Bayesian optimization improved performance: Accuracy increased from 84% to 88%, F1-score from 0.79 to 0.86, and recall from 0.9 to 1.0. These results demonstrate that the model effectively detects all cases of false starts, which is crucial for preventing premature sowing. Across all experiments (see Table 4), the model achieved a **mean accuracy of 0.88±0.16**, a **mean AUC of 0.92±0.18**, and a **mean F1-score of 0.86±0.196**.

5.2 Comparison with Existing Methods Compared to traditional methods such as the Composite Drought Index (CDI) or SMADI, our hybrid approach integrates phenological, climatic, and statistical criteria (Pettitt and Kendall tests), as well as the temporal patterns of precipitation. This allows for a more precise and context-aware detection of false starts, outperforming physical or purely statistical models that struggle to handle climate variability and the multidimensionality of the data. In comparison with recent approaches:

- The IRD model [14], although effective, is limited by the lack of attention mechanisms and low scalability. Our approach integrates multi-source sequences and provides a robust and interpretable solution adapted to Sahelian environments.
- The satellite-based approach by Balti et al. [16] focuses on global drought indices. Our model, by specifically targeting false rainfall starts, adds local value for agricultural planning.
- The model by Ichi et al. [15], based on CAMELS, addresses global hydrological dynamics. Our architecture, optimized for low-resource environments, stands out with fine temporal granularity suited to Sahelian dynamics.
- The Scisimple approach [17] focuses on global seasonal forecasts. Our model complements this work by anticipating short and localized events, which are critical for agricultural decision-making.
- The reference model by Agudelo et al. [18] demonstrates solid performance for predicting USDM categories. In contrast, our approach specifically targets false starts, events absent from these categories, achieving robust performance across 5-fold cross-validation.

Overall, our hybrid model outperforms partial configurations (LSTM alone, LSTM+GRU, etc.) and stands out for its ability to handle the complexity and local variability of the Sahelian climate.

5.3 Limitations Despite the overall improvement in all metrics, certain limitations remain. The complexity of the hybrid model (LSTM + GRU + Transformer) can lead to longer training times and sensitivity to hyperparameter choices. Furthermore, the reliance on the quality and resolution of climate data may affect the robustness of predictions under extreme or unprecedented conditions. These points highlight the need for continuous monitoring and field validation to ensure operational reliability.

5.4 Future Perspectives and Recommendations To further enhance the performance and robustness of the model, efforts should focus on increasing and diversifying the data (including field observations and high-resolution time series), performing field validation to compare predictions with real-world observations, adapting the model regionally to specific climatic and agronomic conditions, and enabling real-time deployment through early warning platforms for farmers and decision-makers. These strategies will maximize the operational applicability and agronomic relevance of false start detection.

6 Conclusion

This work demonstrated the effectiveness of a hybrid model combining LSTM, GRU, and multi-head attention for detecting false starts of the rainy season. Bayesian hyperparameter optimization significantly improved all key metrics, including accuracy, F1-score, and AUC, ensuring reliable and comprehensive detection of critical events. SHAP value analysis enhanced the understanding of the respective contributions of climatic variables, reinforcing the model's transparency and robustness. Despite limitations related to the quality and spatial resolution of the data used, this hybrid approach outperforms traditional methods and shows promising potential for operational deployment as a decision-support tool for agricultural stakeholders. Finally, this work highlights the importance of a continuous improvement approach, based on integrating higher-resolution data and thorough field validation. These steps are essential to optimize the agronomic impact of the model and strengthen the resilience of agricultural systems in the face of increasing climate variability.

References

[1] Muhammad Rasool Al-Kilani, Jawad Al-Bakri, Michel Rahbeh, Cody Knutson, Tsegaye Tadesse, and Qasem Abdelal. Agricultural drought assessment in data-limited arid regions using opensource remotely sensed data: A case study from Jordan. 156(2):89.

[2] Pape ElHadji Abdoulaye Gueye, Cherif Bachir Deme, and Adrien Basse. Improved climate risk assessment tool: Integration of satellite data and machine learning models for climate prediction on farmland around the senegal river. *Mathematical Modelling of Engineering Problems.*, 12(5):1513–1523, May 2025.

[3] Mouhamadou Sylla, Michel Nikiema, Peter Gibba, Ibourahima Kebe, and Nana Ama Browne Klutse. Climate Change over West Africa: Recent Trends and Future Projections. pages 25–40, apr 2016.

[4] Nesrine Farhani. *Contribution of Remote Sensing and Auxiliary Variables in the Study of the Evolution of Drought Periods.* PhD thesis, Université Paul Sabatier - Toulouse III and Université de Carthage (Tunisia), February 2022.

[5] Faye Dioumacor, F Kaly, Abdou Lahat Dieng, Dahirou Wane, Cheikh Modou Noreyni Fall, and Amadou Gaye. Prediction of the Onset and Offset of the Rainy Season in Senegal Using Kohonen Self-Organizing Maps.

[6] Trisha Bhaga, Munyaradzi Shekede, and Cletah Shoko. Impacts of Climate Variability and Drought on Surface Water Resources in Sub-Saharan Africa Using Remote Sensing: A Review. 12:4184.

[7] Kassahun Tenebo Alito, Mulu Sewinet Kerebih, and Dawit Asregedew Hailu. Characterization of Drought Detection With Remote Sensing Based Multiple Indices and SPEI in Northeastern Ethiopian Highland. 18:11786221251328833.

[8] Zhaoxu Zhang, Wei Xu, Zhenwei Shi, and Qiming Qin. Establishment of a comprehensive drought monitoring index based on multisource remote sensing data and agricultural drought monitoring. *IEEE Journal of Selected Topics in Applied Earth Observations and Remote Sensing*, 14:2113–2126, 2021.

[9] Hao Chen, Ni Yang, Xuanhua Song, Chunhua Lu, Menglan Lu, Tan Chen, and Shulin Deng. A novel agricultural drought index based on multi-source remote sensing data and interpretable machine learning. 308:109303.

[10] Zakari Seybou Abdourahamane, Issa Garba, Aboubakr Gambo Boukary, and Alisher Mirzabaev. Spatiotemporal characterization of agricultural drought in the Sahel region using a composite drought index. 204:104789.

[11] Alzira Gabrielle Soares Saraiva Souza, Alfredo Ribeiro Neto, and Laio Lucas de Souza. Soil moisture-based index for agricultural drought assessment: SMADI application in pernambuco state-brazil. 252:112124, 2021.

[12] Rajkumar Guria, Manoranjan Mishra, Richarde Marques da Silva, and Carlos Antonio Costa dos Santos. Multisensor Integrated Drought Severity Index (IDSI) for assessing agricultural drought in Odisha, India. 37:101399.

[13] Mikhael G. Alemu and Fasikaw A. Zimale. Integration of remote sensing and machine learning algorithm for agricultural drought early warning over Genale Dawa river basin, Ethiopia. 197(3):243.

[14] Seyni Salack, Koufanou Hien, Namo K. Z. Lawson, Inoussa Abdou Saley, Jean-Emmanuel Paturel, and Moussa Waongo. Prévisibilité des faux-départs de saison agricole au sahel. In *Risques climatiques et agriculture en Afrique de l'Ouest*, pages 31–43. IRD Éditions, 2025. Consulté en août 2025.

[15] 500daysofAI. Prédire les inondations et la sécheresse avec l'ia, 2025. Synthèse d'un article NeurIPS 2019 sur les LSTM appliqués aux bassins versants via le jeu de données CAMELS.

[16] Hanen Balti, Raja Inoubli, Ali Ben Abbes, and Riadh Farah. Prédiction de la sécheresse à partir des images satellitaires : une approche à base d'apprentissage profond. In *Actes de la conférence TAIMA 2022*, 2022.

[17] Simple Science. Exploiter l'apprentissage automatique pour prédire les pluies saisonnières en afrique de l'est, 2025. Consulté en août 2025. Résumé d'une étude sur l'utilisation de LASSO et Elastic Net pour la prévision pluviométrique saisonnière en Afrique de l'Est.

[18] Julian Agudelo, Vincent Guigue, Cristina Manfredotti, and Hadrien Piot. Prévision de sécheresse en utilisant une architecture neuronale hybride intégrant des séries temporelles et des données statiques. In *Conférence hébergée de l'AFIA*, 2025.

[19] Sepp Hochreiter and Jürgen Schmidhuber. Long Short-Term Memory. *Neural Comput.*, 9(8):1735–1780, nov 1997.

[20] Krzysztof Zarzycki and Maciej Ławryńczuk. Advanced predictive control for gru and lstm networks. *Information Sciences*, 616:229–254, 2022.

Declarations

Funding: No funding was received for conducting this study. **Conflicts of interest:** The authors declare no conflict of interest. **Data availability:** Dataset available upon reasonable request. **Ethical approval:** Not applicable for this computational study.